

Influence of point defects in KTaO_3 on low-temperature dielectric relaxation

Anna-Karin Axelsson^a, Matjaz Valant^{a,b,*}, Neil McN. Alford^a

^a Department of Materials, Imperial College London, Exhibition Road, London SW7 2AZ, UK

^b Materials Research Laboratory, University of Nova Gorica, Vipavska 13, 5000 Nova Gorica, Slovenia

Received 4 August 2009; received in revised form 23 September 2009; accepted 30 September 2009

Available online 4 November 2009

Abstract

Substituted KTaO_3 ceramics were synthesized, sintered and studied using low-temperature microwave dielectric analysis and Raman spectroscopy. Because of a fundamentally different nature of aliovalent Mn- and isovalent Na-substitution mechanisms, significant differences in processing and dielectric properties were identified. The properties were correlated to the defect structure of the substituted KTaO_3 lattices. Characteristics of the induced polar domains were clearly different for the two substitutional mechanisms, which further reflects in a significantly different dielectric behavior. Linear response of changes in the Raman spectra corresponds to evidence of the formation of symmetry-breaking regions.
© 2009 Elsevier Ltd. All rights reserved.

Keywords: Defects; Dielectric properties; Ferroelectric properties; Tantalates; Polar domains

1. Introduction

KTaO_3 is an incipient ferroelectric and displays a continuous increase in the dielectric constant with decreasing temperature. KTaO_3 exhibits many technologically interesting properties. It can be used in optoelectronics for optical waveguides. In combination with low-loss superconductors it has been considered for applications in tunable microwave components and fatigue-free nonvolatile memories.¹ Additionally, it possesses a combination of a high permittivity and relatively low dielectric losses at room temperature, which makes it an attractive candidate for application in microwave devices.² It exhibits semiconductor properties with a band gap suitable for photocatalytic water splitting.³ In many applications it is used in a form of powders and single crystals but ceramic elements are frequently required to reduce production and machining cost, increase design flexibility and functionality. Sintering of KTaO_3 powder is very difficult mainly due to the high covalent bonding within this crystal structure.^{4,5} More effective sintering has been obtained with an aid of dopants.^{6,7} However, the dopants can significantly change functional properties (e.g. optical and dielectric) and can-

not be tolerated for particular applications. Especially sensitive to the presence of dopants are dielectric properties. The presence of additional polarization mechanisms can significantly alter the dielectric relaxation processes in such a material. Consequently, this can result in a significant increase in dielectric losses and a reduced technological value of the material.

One type of defect that occurs at aliovalent substitutions is dipoles, generated by e.g. a Columbic attraction of oppositely charged species. This type of random lattice disorders would cause a dielectric anomaly and pronounced relaxation when exposed to an electromagnetic field. Most commonly, this type of local ferroelectric phase transition is induced by different types of defect such as local symmetry-breaking defects (SB) or the soft non-symmetry-breaking (NSB) defects that increase the local ferroelectric transition temperature.⁸ Raman spectroscopy and inelastic neutron scattering studies have revealed the effect of the oxygen vacancies on the ferroelectric soft mode in reduced SrTiO_3 . Similar results have been obtained for KTaO_3 .⁹ In these cases, the oxygen vacancies act as very hard local NSB defects, which affect the local ferroelectric transition temperature.

In practice this may mean that for polycrystalline substituted KTaO_3 systems, the physics, which is governing the behavior of the single crystals, is changed. By solid state synthesis, deviation of the phonon fluctuations comes from a number of sources including grain boundaries, impurities, vacancies. Therefore, the dielectric loss, especially in low temperatures, is linked to

* Corresponding author at: University of Nova Gorica, Vipavska 13, 5000 Nova Gorica, Slovenia. Tel.: +386 53653502; fax: +386 53653527.

E-mail address: matjaz.valant@ung.si (M. Valant).

mixing of the modes not observed in very high quality single crystals.¹⁰ The information about the interaction between the low frequency modes can be obtained directly by Raman spectroscopy, far infrared spectroscopy and indirectly by dielectric measurements.

In the present contribution we will report on our investigations of these phenomena. We compare pure KTaO_3 with isovalently and aliovalently doped KTaO_3 , in which point defect such as substitutional ions, off-centering and vacancies are present. Low-temperature dielectric measurements that were performed on these samples gave us a tool to associate these point defects to appearance of polarons and polar nano-domains. These were further correlated to the observed changes in the relaxation processes.

2. Experimental

Starting powders of K_2CO_3 (99.9% BDH AnalaR), Ta_2O_5 (99.995% Pi-Kem Ltd.) MnO_2 and Na_2CO_3 (both Alfa Aesar 99.9%) were carefully dried prior to stoichiometric mixing. The mixture was homogenised by dry ball milling using yttria-stabilized zirconia balls, pressed into pellets (13 mm stainless steel die, 100 MPa) and fired in a muffle furnace in an air atmosphere. The progress of the reaction was monitored by X-ray diffractometry (Philips X'pert Pro) Cu K_α radiation and high throughput detector (X'Celerator, Philips Analytical) equipped with diffracted beam monochromator. The fraction of the phases formed during the reaction was estimated from peak integrals on normalized X-ray scans. The processes occurring during heat treatment were evaluated with thermo-gravimetry (TG), differential thermal analysis (DTA) and evolved gas analysis (EGA) (Netzsch STA 449C) system coupled to a quadrupole mass spectrometer. The microstructures were examined using scanning electron microscope (JEOL 840A) and INCA 4.07 (Oxford Instruments) software.

The characteristics of sintering were examined using a dilatometer (Netzsch 402C). The pellets were then placed in a dilatometer and heated to a temperature of 1360 °C at a heating rate of 5 °C/min. Based on the obtained sintering curves the optimum sintering conditions were selected. Density was evaluated by measuring dimensions and mass of the sintered samples.

Microwave measurements were carried out on a Vector Network Analyser (Agilent HP8720C) with 1 Hz resolution using a silver coated high-purity copper cavity. The TE_{018} fundamental mode was used for measurement in transmission mode. This resonance mode was used due to its high electric energy filling factor. The measurements were performed on sintered pucks with approximately 10.7 mm in diameter and 2.5–3.5 mm in height. The corresponding resonant frequency at room temperature was always between 2.5 and 3.5 GHz and varied as a consequence of the temperature dependence of the relative permittivity. To reduce conduction losses the samples were placed on a low-loss small diameter quartz post. The cavity assembly was placed on a cold-head of a two-stage Gifford-McMahon cryo-cooler (Cryophysics, Abingdon, U.K.), which operates over a temperature range 10–320 K. All measurements started with initial 30 min temperature stabilization at 15 K, fol-

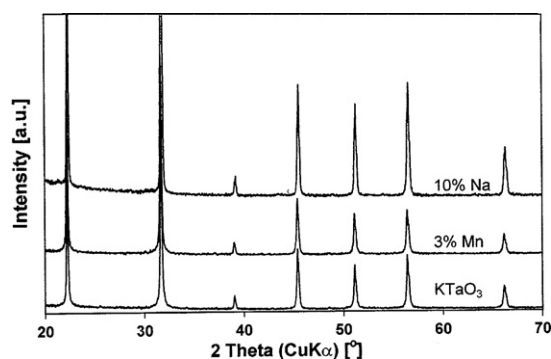


Fig. 1. XRD patterns of KTaO_3 , $\text{K}_{0.94}\text{Mn}_{0.03}\text{TaO}_3$ and $\text{K}_{0.90}\text{Na}_{0.10}\text{TaO}_3$ powders calcined at 950 °C for 5 h.

lowed by a ramp up of 1 K/min. Resonant frequency, insertion loss and loaded Q were measured at small temperature intervals. In-house written software^c was used for an accurate evaluation of unloaded Q and relative permittivity based on radial mode matching technique.¹¹

Raman spectra from the sintered optical polished pucks were recorded using a MicroRaman Spectrometer (Renishaw System 2000) with a 514 nm line of an Ar^+ laser as exciting radiation with nominally <4 mW power incident on the sample surface. The laser line was focused onto the sample by a cylindrical microscope lens of 50× magnification with a spot diameter of $2 \pm 1 \mu\text{m}$.

3. Results

Three different KTaO_3 -based materials were synthesized for this study: pure KTaO_3 , Na- and Mn-substituted KTaO_3 . K ions were isovalently substituted by Na ions according to the formula $(\text{K}_{1-x}\text{Na}_x)\text{TaO}_3$ or aliovalently by Mn ions according to $(\text{K}_{1-2x}\text{Mn}_x\text{□}_x)\text{TaO}_3$, where \square represents vacancies on A-site of the perovskites. The incorporation of Mn^{2+} has been a subject of many detailed investigation. Although early investigations suggested on partial Mn^{2+} incorporation onto B-site and creation of $\text{Mn}^{2+}-\text{V}_\text{O}$ centers¹² the new results have confirmed the substitution of potassium without formation of $\text{Mn}^{2+}-\text{V}_\text{O}$ centers, i.e. the stoichiometry that we adopted in this paper. It has been established that electronic/orbital interactions in Mn-doped KTaO_3 cause the dopant Mn^{2+} ions to off-center along the [1 0 0] direction from the potassium Wyckoff $1b$ position for as much as 0.9 Å.^{13–15} This means that the Mn^{2+} ion occupies a position somewhat in the middle of the adjacent oxygen planes and can be regarded as a sort of Frenkel defect.⁷

We studied the sample with 10% Na-substitution, for which the synthesis yielded a single-phase reaction product (Fig. 1). In the case of Mn we could not use the sample with 10% substitution because the substitution limit is low, ~4%. We performed the studies on $(\text{K}_{0.98}\text{Mn}_{0.01})\text{TaO}_3$ and $(\text{K}_{0.94}\text{Mn}_{0.03})\text{TaO}_3$, for which a single-phase material was obtained after calcination at 950 °C/5 h. For a direct comparison of the dielectric relaxation

^c The software was written by Jonathan Breeze, Department of Materials, Imperial College London.

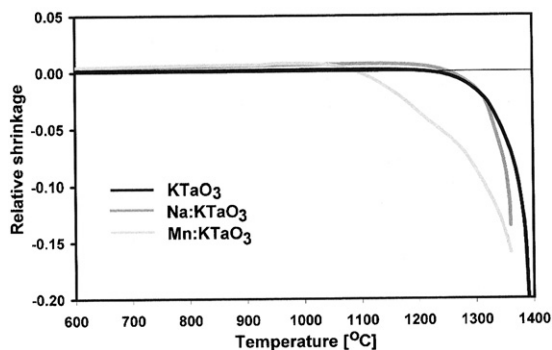


Fig. 2. Sintering curves of KTaO_3 , $\text{K}_{0.94}\text{Mn}_{0.03}\text{TaO}_3$ and $\text{K}_{0.90}\text{Na}_{0.10}\text{TaO}_3$ powders (average particle size $<1\ \mu\text{m}$, heating rate $5^\circ\text{C}/\text{min}$).

phenomena it is important to notice that the XRD patterns of all three studied KTaO_3 -based materials show no changes in the crystal symmetry.

After calcination the powders were milled to an average particle size of $<1\ \mu\text{m}$. The sintering curves of such powders are shown in Fig. 2. It is clear that the isovalent substitution does not change the sintering kinetics but the aliovalent substitution makes a significant difference. The difference comes from the increased concentration of vacancies that promote lattice diffusion and so, improves the sintering kinetics. The optimum sintering temperature was chosen to be 1350°C for pure and Na-substituted KTaO_3 , and 1330°C for Mn-substituted KTaO_3 . The relative densities obtained after the sintering were in the range of 80–85%. Typical microstructures are shown in Fig. 3.

The dielectric response varies with the nature of the substituents as shown in Fig. 4. The slope of the $\epsilon_r(T)$ plot of pure KTaO_3 reflects the soft-mode driven increase of permittivity that follows Curie Weiss law.⁴ At 20 K, the slope of permittivity is $-2.4\%/K$. When substituting with 10%Na the slope does not change significantly reaching a value of $-2.1\%/K$ whereas a tenth of that amount of Mn substitution reduces the slope to $-1.2\%/K$. This proves that the polar nano-domain fluctuations formed by aliovalent substitution have a greater impact on the dielectric response.

The same conclusion comes from comparing $\tan\delta(T)$ plots. Although the Mn substitution is only a fraction of the Na-substitution a huge difference in the loss spectrum can be observed. The most striking difference is that in both, pure and Na-substituted KTaO_3 , a remarkable increase in loss occurs when approaching T_c at temperatures below 50 K. This is in agreement with the permittivity plot and indicates that the hardening of the soft mode may not be significant when substituting with Na.

When substituting with Mn^{2+} , there is no increase of $\tan\delta$ when approaching 0 K. This suggests that the polar nano-domains that are formed at aliovalent substitution have a large impact on the soft mode. The conclusion is also supported by the observed large decrease in the $\epsilon_r(T)$ slope. In addition, two distinct loss regions are observed at 120 and 230 K, where the latter appears to be of a very complex nature and most probably consists of several superimposed peaks referred to earlier.⁷

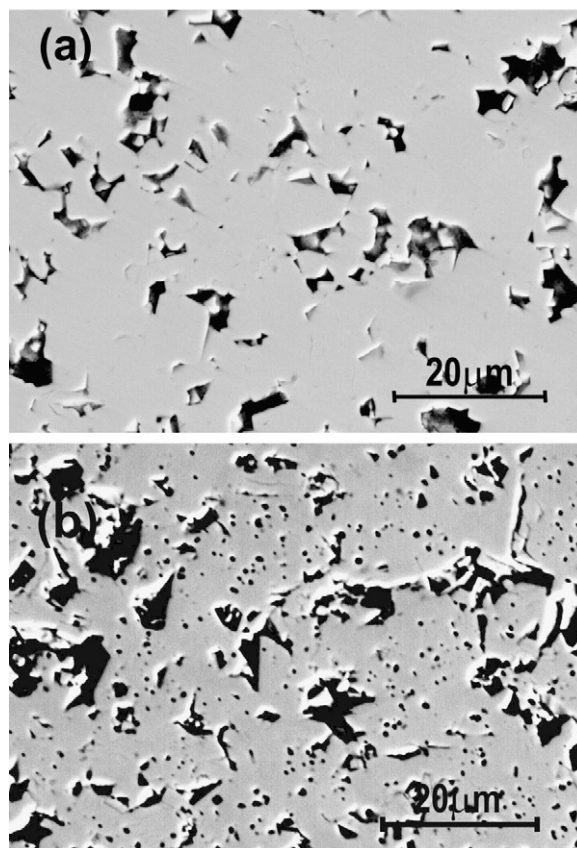


Fig. 3. Backscattered electron image of (a) typical KTaO_3 , and $\text{K}_{0.90}\text{Na}_{0.10}\text{TaO}_3$ microstructure after sintering at 1350°C for 1 h and (b) typical $\text{K}_{0.94}\text{Mn}_{0.03}\text{TaO}_3$ microstructure after sintering at 1330°C for 1 h.

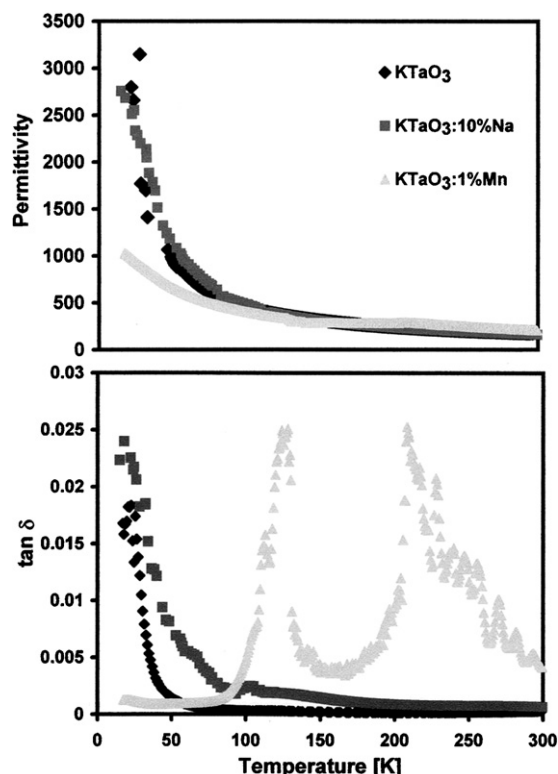


Fig. 4. Temperature dependence of microwave dielectric properties of KTaO_3 , $\text{K}_{0.90}\text{Na}_{0.10}\text{TaO}_3$ and $\text{K}_{0.98}\text{Mn}_{0.01}\text{TaO}_3$.

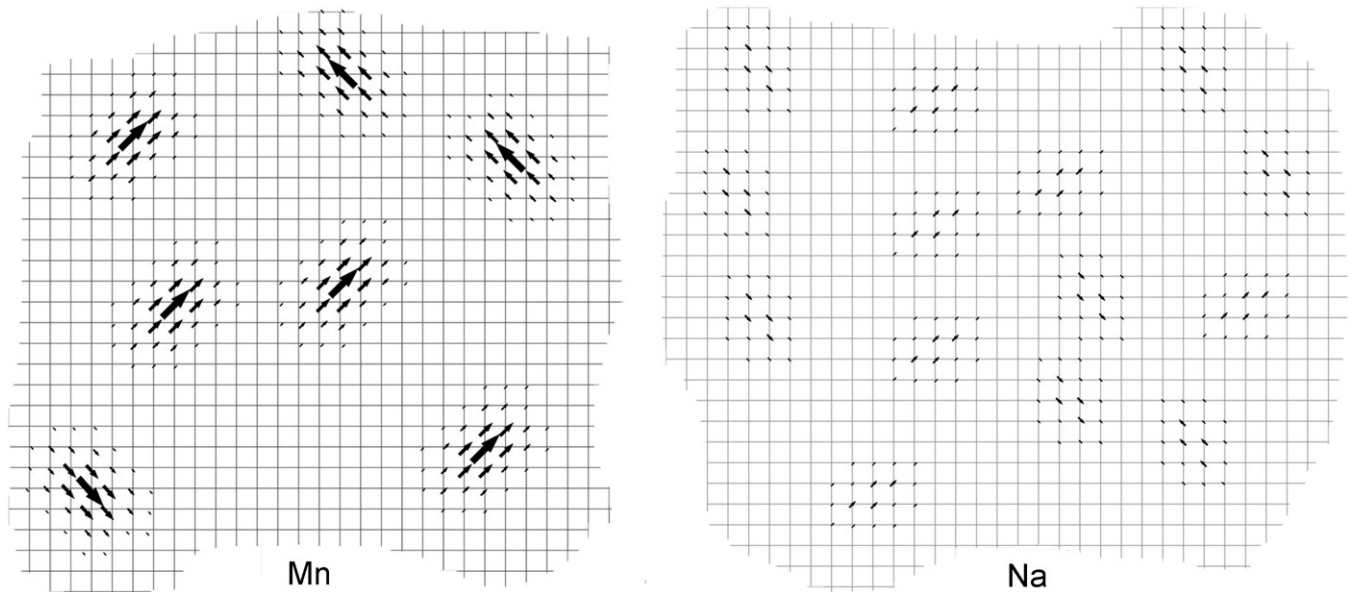


Fig. 5. Schematic presentation of polar nano-domains induced by the aliovalent Mn- and isovalent Na-substitution.

4. Discussion

For the both types of substitution some off-centering of the dopant ion is present. However, because of a significantly different mode and degree of the off-centering we expect a significant different polar contribution to the dielectric properties.

In 1% Mn-substituted KTaO_3 , there is effectively one additional vacancy induced polaron per 100 unit cell. This will form polar domains with their own activation energy, fluctuation mechanism and oscillation characteristics over temperature (Fig. 5). Given that the correlation length between the polarons increases inversely with temperature a significantly different dielectric response is expected for aliovalent substitution.

The substitution of larger K^+ with smaller Mn^{2+} ion ($\text{Mn}_{(\text{extrapolated to CN}=12)}^{2+} \sim 1.27 \text{ \AA}$ and $\text{K}_{(\text{CN}=12)}^+ = 1.64 \text{ \AA}$)¹⁶ also induces a large displacement (0.9 \AA) and local tetragonal symmetry.^{13–15} This local symmetry distortion has been associated with the large Mn displacement rather than to the charge compensation and cation vacancy appearance, which may only occur in distant ligand spheres. In the case of Na^+ substitution (1.39 \AA for $\text{CN}=12$) some local symmetry change would also be expected due to a slight Na off-centering.¹⁷ The physics behind the fluctuations of Na displacement is not well understood but most likely the fluctuation at cryogenic temperatures originates from ion hopping among several Na equivalent positions, it is probably that their fluctuations are either frozen out before their correlation length becomes large enough to play a significant role or simply their activation energy and dipole strength is too low. Hence, no significant hardening of the soft mode is observed.

Using Raman spectroscopy we can probe the lattice distortions as pure KTaO_3 is cubic and therefore no first-order Raman scattering is observed. Raman spectroscopy is a sensitive probe for polar correlations and KTaO_3 has often been used as a model system to study the soft-mode behavior and phonon–phonon interaction over temperature ranges.¹⁸ The ferroelectric soft

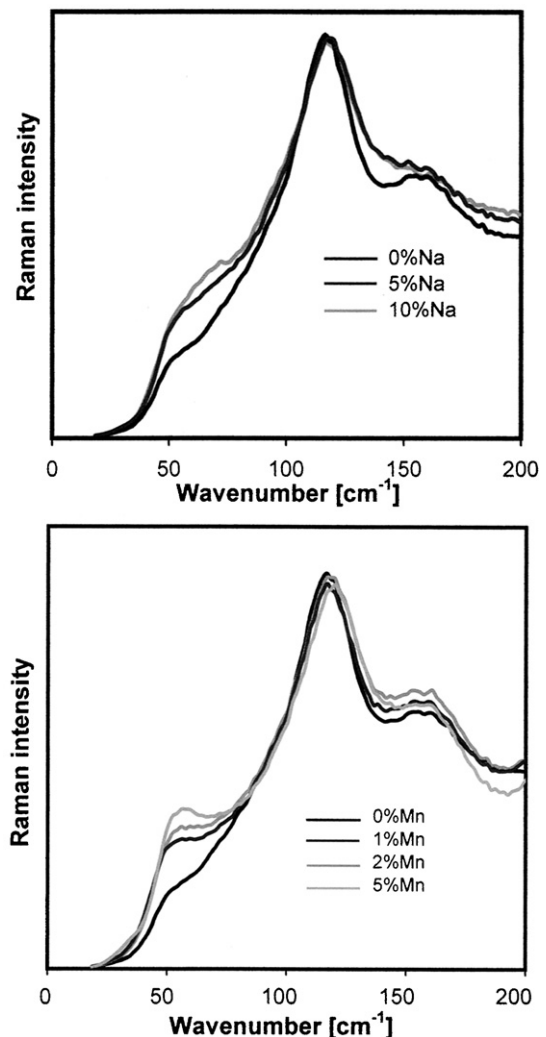


Fig. 6. Raman spectra for (a) Mn- and (b) Na-substituted KTaO_3 ceramics with different amount of substitution.

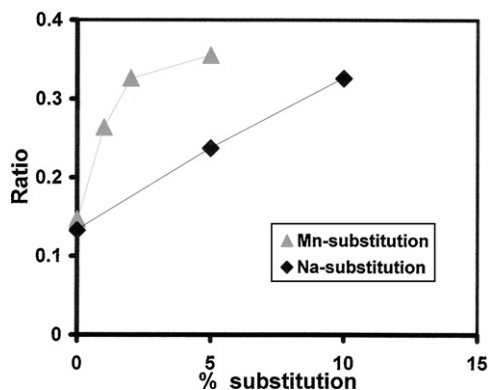


Fig. 7. The intensity of the parent 55 cm^{-1} Raman mode for Mn- and Na-substituted KTaO_3 as a function of amount of substitution.

mode originates from anisotropic O^{2-} polarizability in the O–Ta–O lattice vibration in a pure KTaO_3 . Furthermore, this anisotropic polarization is responsible for a powerful second order Raman scattering observed in KTaO_3 . It has been argued that these strong secondary modes mask changes caused by substitutions at room temperature and such changes can only be observed at low temperatures where a type of local ferroelectric transition occurs. Our results of the Raman response, shown in Fig. 6, clearly confirm a difference between the parent, isovalent and aliovalent substituted KTaO_3 .

We focused the attention to modes below 190 cm^{-1} as we believe that the expected symmetry breaks form a phonon-scatter of the first-order due to the introduction of substituent of different average mass and atomic positions. In pure KTaO_3 the first-order (zone-center) modes are forbidden. However, based on our dielectric studies of KTaO_3 ceramics we can suggest that even in a nominally pure KTaO_3 ceramics there are regions that cause relaxor-like behavior due to their polar nature. We noticed that in ceramics these structural defects and their manifestation in dielectric spectra are much more pronounced than in single crystals.¹⁹ In particular, we noted that during prolonged annealing potassium loss occurs and a tungsten–bronze secondary phase appears⁴ and these are indicators of oxygen deficiency and grain boundary defects. Such samples would potentially show first-order modes despite formally being forbidden for KTaO_3 symmetry. Moreover, when comparing the Raman response between ceramics and a single crystal, strict selection rules cannot be followed because of higher dampening of the phonon vibrations in ceramics and mixing of the modes, which in single crystals is not allowed.¹⁰

In “pure” KTaO_3 ceramics a small shoulder at around 55 cm^{-1} is visible. The origin of the mode is not clear except that it may correspond to the above-mentioned evidence of structural disorders observed in ceramics. The most striking is the direct response of this peak to Mn substitution (see Fig. 6).

Here we can clearly see a direct Raman response of the Mn substitution, which can only be regarded as a new type of first-ordered response due to introduction of several symmetry-breaking factors such as (a) Mn^{2+} off-centering, (b) variation in atomic mass on the A-site and (c) cation vacancies. The increase of the 55 cm^{-1} peak slows down over 3% substitution (Fig. 7),

which is in agreement with our evidence for the solid solubility limit of Mn^{2+} in KTaO_3 .⁷ The Raman response is also evident but not strong for Na-substitution. There seems to be a slight dampening and increase in the 55 cm^{-1} mode. The development of the symmetry breaks is not expected to be so strong for this isovalent substitution as Na only slightly off-centers from the A-site, the atomic mass is very similar to K and no additional vacancies are formed.

5. Conclusions

The study demonstrated the significant influence of substitution mechanisms on the properties of KTaO_3 . The major influence comes from different defect structures of the substituted KTaO_3 lattice. The aliovalent Mn substitution induces large Mn^{2+} off-centering, strong variation in atomic mass on the A-site, cation vacancies whereas the isovalent Na-substitution induces only slight off-centering and negligible variation in atomic mass. The sintering of Mn-substituted KTaO_3 is enhanced because of a higher concentration of vacancies. The characteristics of the soft mode are significantly influenced by a strong coupling of the polar nano-domains in the Mn-substituted KTaO_3 resulting in low permittivity and dielectric loss at cryogenic temperatures. In addition, two distinct loss regions are observed at 120 and 230 K. Because of the far lower level of distortion of the Na-substituted lattice the properties remain similar to those of the parent KTaO_3 . The Raman studies confirmed a difference between the parent, isovalent and aliovalent substituted KTaO_3 and are in agreement with the assumed substitutional mechanism and the expected lattice distortion.

References

- Boikovb, A. Y., Ivanov, Z. G., Olsson, E. and Claeson, T., Epitaxial ferroelectric/superconductor heterostructures. *Physica C*, 1997, **111**, 282–287.
- Geyer, R. G., Riddle, B., Krupka, J. and Boatner, L. A., Microwave dielectric properties of single-crystal quantum paraelectrics KTaO_3 and SrTiO_3 at cryogenic temperatures. *J. Appl. Phys.*, 2005, **97**, 104–111.
- Ishihara, T., Nishiguchi, H., Fukamachi, K. and Takita, Y., Effects of acceptor doping to KTaO_3 on photocatalytic decomposition of pure H_2O . *J. Phys. Chem. B*, 1999, **103**(1), 1–3.
- Axelsson, A.-K., Pan, Y., Valant, M. and Alford, N. M., Synthesis, sintering, and microwave dielectric properties of KTaO_3 ceramics. *J. Am. Ceram. Soc., Early View*, 2009(June).
- Chen, Z. X., Zhang, X. I. and Cross, L. E., Low-temperature dielectric-properties of ceramic potassium tantalate (KTaO_3). *J. Am. Ceram. Soc.*, 1983, **66**, 511–515.
- Shimada, S., Kodaira, K. and Matsushita, T., Sintering LiTaO_3 and KTaO_3 with the aid of manganese oxide. *J. Mater. Sci.*, 1984, **19**, 1385–1390.
- Axelsson, A.-K., Pan, Y., Valant, M. and Alford, N.M., Chemistry, processing and microwave dielectric properties of Mn-substituted KTaO_3 ceramics. *J. Am. Ceram. Soc.*; in press.
- Smolyaninov, I. M. and Glinchuk, M. D., The role of the oxygen vacancies in formation of low temperature state in the quantum paraelectrics SrTiO_3 and KTaO_3 . *J. Korean Phys. Soc.*, 1998, **32**, S400.
- Jandl, S., Banville, M., Dufour, P., Coulombe, S. L. and Boatner, L. A., Infrared study of oxygen vacancies in KTaO_3 . *Phys. Rev. B*, 1991, **43**, 7555–7560.
- Dunne, L. J., Axelsson, A.-K., Alford, N. M., Breeze, J., Aupi, X. and Brändas, E. J., Quasi-classical fluctuation-dissipation description of dielectric

- loss in oxides with implications for quantum information processing. *Int. J. Quantum Chem.*, 2006, **106**, 986–993.
11. Kajfez, D. and Guillon, P., *Dielectric Resonator*. Artech House, Dedham, USA, 1986.
 12. Bykov, I. P., Geifman, I. N., Glinchuk, M. D. and Krulikovskii, B. K., Electron-paramagnetic-res study of Mn^{2+} -vacancy dipole reorientation in $KTaO_3$. *Fiz. Tverd. Tela (Leningrad)*, 1980, **22**, 2144–2148; Bykov, I. P., Geifman, I. N., Glinchuk, M. D. and Krulikovskii, B. K., Electron-paramagnetic-res study of Mn^{2+} -vacancy dipole reorientation in $KTaO_3$. *Trans. Sov. Phys. Solid State*, 1980, **22**, 1248.
 13. Siegel, E. and Muller, K. A., Structure of transition-metal–oxygen–vacancy pair centers. *Phys. Rev. B*, 1979, **19**, 109–120.
 14. Laguta, V. V., Glinchuk, M. D., Bykov, I. P., Rosa, J., Jastrabik, L., Savinov et al., Paramagnetic dipole centers in $KTaO_3$: electron-spin-resonance and dielectric spectroscopy study. *Phys. Rev. B*, 2000, **61**, 3897–3904.
 15. Venturini, E. L., Samara, G. A., Laguta, V. V., Glinchuk, M. D. and Kondakova, I. V., Dipolar centers in incipient ferroelectrics: Mn and Fe in $KTaO_3$. *Phys. Rev. B*, 2005, **71**, 094111.
 16. Shannon, R. D., Revised effective ionic radii and systematic studies of interatomic distances in halides and chalcogenides. *Acta Crystallogr.*, 1976, **A32**, 751–767.
 17. Maglione, M., Rod, S. and Höchli, U. T., Order and disorder in $SrTiO_3$ and in pure and doped $KTaO_3$. *Europhys. Lett.*, 1987, **4**, 631–636.
 18. Perry, C. H., Currat, R., Buhay, H., Migoni, R. M., Stirling, W. G. and Axe, J. D., Phonon-dispersion and lattice-dynamics of $KTaO_3$ from 4 K to 1220 K. *Phys. Rev. B*, 1989, **39**(12), 8666–8676.
 19. Samara, G. A., The relaxation properties of compositionally disordered ABO_3 perovskites. *J. Phys.: Condens. Matter*, 2003, **15**, R367–R411.